Structural and Functional Diversities among μ-Conotoxins Targeting TTX-resistant Sodium Channels†

Min-Min Zhang,‡ Brian Fiedler,‡ Brad R. Green,‡ Phillip Catlin,‡ Maren Watkins,§ James E. Garrett,‖ Brian J. Smith,⊥ Doju Yoshikami,‡ Baldomero M. Olivera,‡ and Grzegorz Bulaj*,‡

Departments of Biology and Pathology, University of Utah, Salt Lake City, Utah, 84112, Cognetix, Inc., 421 Wakara Way, Suite 201, Salt Lake City, Utah, 84108, and The Walter and Eliza Hall Institute of Medical Research, 1G Royal Parade, Parkville 3050, Australia

Received October 22, 2005; Revised Manuscript Received January 12, 2006

ABSTRACT: μ-Conotoxins are peptides that block sodium channels. Molecular cloning was used to identify four novel μ-conotoxins: CnIIIA, CnIIIB, CIIIA, and MIIIA from *Conus consors*, *C. catus* and *C. magus*. A comparison of their sequences with those of previously characterized μ-conotoxins suggested that the new μ-conotoxins were likely to target tetrodotoxin-resistant (TTX-r) sodium channels. The four peptides were chemically synthesized, and their biological activities were characterized. The new conotoxins all blocked, albeit with varying potencies, TTX-r sodium currents in frog dorsal-root-ganglion (DRG) neurons. The more potent of the four new μ-conotoxins, CnIIIA and CIIIA, exhibited a strikingly different selectivity profile in blocking TTX-r versus TTX-sensitive channels, as determined by their ability to block extracellularly recorded action potentials in three preparations from frog: skeletal muscle, cardiac muscle and TTX-treated C-fibers. CnIIIA was highly specific for TTX-r sodium channels, whereas CIIIA was nonselective. Both peptides appeared significantly less potent in blocking TTX-r sodium currents in rat and mouse DRG neurons. When CnIIIA and CIIIA were injected intracranially into mice, both induced seizures, but only CIIIA caused paralysis. This is the most comprehensive characterization to date of the structural and functional diversities of an emerging group of μ-conotoxins targeting TTX-r sodium channels.

The molecular diversity of voltage-gated sodium channels is reflected by the numerous isoforms of these channels and suggests that they play distinct roles in the central and peripheral nervous systems (*1, 2*). Sodium channels have been implicated in a number of pathophysiological conditions, including genetic or acquired channelopathies and neuropathic pain (*3*−*6*). There is a widespread effort to discover and develop subtype-selective sodium channel antagonists. One promising source of potential new ligands that target sodium channels is natural toxins (*7*).

Conotoxins found in venoms of predatory cone snails have proven to be a rich source of ligands targeting numerous receptors and voltage-gated ion channels (*8*). Three families of conotoxins, namely μ-, μO-, and δ-conotoxins, target sodium channels. μ-Conotoxins and μO-conotoxins block sodium channels, whereas δ-conotoxins inhibit channel inactivation (Figure 1). Despite the initial discovery of μO-conotoxins MrVIA and MrVIB a decade ago (9), no new members of this conotoxin family have been isolated or characterized. However, multiple molecular forms of μ-conotoxins have been discovered (Table 1). The first μ-conotoxins that were characterized (GIIIA, GIIIB, and GIIIC) were isolated from *Conus geographus* venom. These peptides induced paralysis in fish and mice and were shown to target skeletal-muscle sodium channels ($Na_V1.4$) with high potency (*10*, *11*).

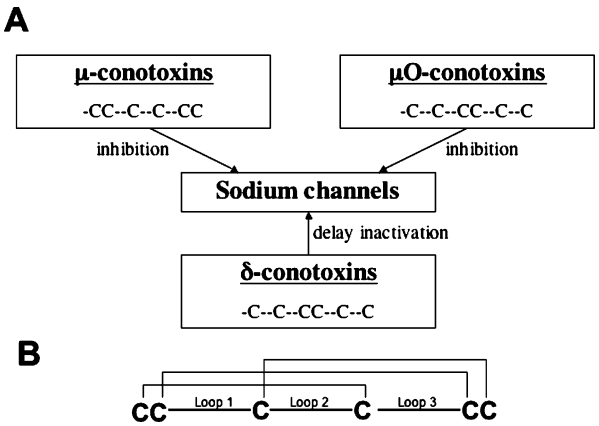

FIGURE 1: (A) Overview of conotoxin families targeting sodium channels. Two families, μ- and μO-conotoxins inhibit sodium channels, whereas δ-conotoxins delay channel inactivation. (B) Diagram illustrating disulfide-bridge connectivity in μ-conotoxins, resulting in three loops. Note that the arrangement of six cysteines differs between μ- and μO-conotoxins: the latter have four, rather than three loops. The disulfide-bridge connectivity is identical for both μ- and μO-conotoxins: CysI−CysIV, CysII−CysV, and CysIII−CysVI.

Characterization of μ-PIIIA from *Conus purpurascens*, which primarily targeted $Na_V1.4$ (IC_{50} ∼40 nM), revealed

† This work was supported by National Institutes of Health grant GM 48677 to B.M.O. and D.Y., from the National Institute of General Medical Sciences. B.J.S. acknowledges support from the NHMRC..

* To whom correspondence should be addressed. E-mail bulaj@biology.utah.edu. Tel: (801) 581-8370. Fax: (801) 585-5010.

‡ Department of Biology, University of Utah.

§ Departments of Pathology, University of Utah.

‖ Cognetix, Inc.

⊥ The Walter and Eliza Hall Institute of Medical Research.

10.1021/bi052162j CCC: $33.50
Published on Web 02/24/2006

Table 1: Structures and Activities of μ-Conotoxins[a]

conotoxin	structure[b]	activity[d]	reference
Group I			
CnIIIA	GR**CC**DVPNA**C**SGRW**C**RDHAQ**CC**[b]	TTX-r	this work
CnIIIB	ZG**CC**GEPNL**C**FTRW**C**RNNAR**CC**RQQ[c]	TTX-r	this work
MIIIA	ZG**CC**NVPNG**C**SGRW**C**RDHAQ**CC**[b]	TTX-r	this work
CIIIA	GR**CC**EGPNG**C**SSRW**C**KDHAR**CC**[b]	TTX-r, TTX-s	this work
Group II			
SmIIIA	ZR**CC**NGRRG**C**SSRW**C**RDHSR**CC**[b]	TTX-r, TTX-s	(*14*)
SIIIA	ZN**CC**NG--G**C**SSKW**C**RDHAR**CC**[b]	TTX-r	(*16*)
KIIIA	**CC**N----**C**SSKW**C**RDHSR**CC**[b]	TTX-r	(*16*)
Group III			
PIIIA	ZRL**CC**GFOKS**C**RSRQ**C**KOH-R**CC**[b]	$Na_v1.4$, $Na_v1.2$	(*12, 33*)
GIIIA	RD**CC**TOOKK**C**KDRQ**C**KOQ-R**CC**A[b]	$Na_v1.4$	(*10*)
GIIIB	RD**CC**TOORK**C**KDRR**C**KOM-K**CC**A[b]	$Na_v1.4$	(*10*)
GIIIC	RD**CC**TOOKK**C**KDRQ**C**KOL-K**CC**A[b]	$Na_v1.4$	(*10*)

[a] The three loops and the connectivity of disulfide bridges are illustrated in Figure 1B. [b] *C*-terminal amidation. [c] *C*-terminal free acid, *O*,4-*trans*-hydroxyproline. [d] The activities of μ-conotoxins in groups I and II were determined using frog preparations, whereas those in group III were determined largely with cloned sodium channels from rat.

that it exhibited some activity toward the neuronal sodium channel subtype Na_V 1.2 (IC_{50} ~690 nM) (*12*, *13*). Recently, our group discovered three new μ-conotoxins, namely SmIIIA, SIIIA, and KIIIA that blocked TTX-resistant (TTX-r)[1] channels and had different potencies against TTX-sensitive channels (*14*−*16*). Although 1 μM SmIIIA blocked TTX-sensitive action potentials in skeletal muscle by 70%, 1 μM of either KIIIA or SIIIA had hardly any effect (*16*). It thus appears that μ-conotoxins are a source of pharmacological agents for Na channels of considerable potential.

In a continuing effort to discover and characterize μ-conotoxins that have novel sodium-channel subtype specificity, we utilized a combination of molecular cloning, cladistic analysis, and chemical synthesis. This approach has already proven to have some success for this family of toxins, with KIIIA and SIIIA being the first natural toxins shown to preferentially block TTX-resistant sodium channels in DRG neurons over TTX-sensitive channels in skeletal muscle. Here, we describe four new μ-conotoxins from fish-hunting cone snails that share considerable sequence homology. These conotoxins were chemically synthesized, and their biological activities were examined. The data provides insight into the structure−function relationships of conotoxins targeting TTX-resistant sodium channels.

[1] Abbreviations: ACN, acetonitrile; CAP, compound action potential; DRG, dorsal root ganglion; Fmoc, *N*-(9-fluorenyl)methoxycarbonyl; MTBE, methyl-tert butyl ether; KIIIA, μ-conotoxin KIIIA; PCR, polymerase chain reaction; SIIIA, μ-conotoxin SIIIA; SmIIIA, μ-conotoxin SmIIIA; TFA, trifluoroacetic acid; Trt, trityl; TTX, tetrodotoxin; TTX-r, tetrodotoxin-resistant.

EXPERIMENTAL PROCEDURES

Cloning of Conotoxins

PCR amplification, construction of cDNA libraries, and cloning of μ-conotoxins were performed as described previously (*14*, *16*).

Chemical Synthesis of Conotoxins

Synthetic conotoxins were produced using methods identical to those described previously (*16*). Briefly, the peptides were synthesized on solid support using standard Fmoc (*N*-(9-fluorenyl)methoxycarbonyl) chemistry. The peptides were cleaved from the resin by a 3−4 h treatment with reagent K (trifluoroacetic acid (TFA)/water/ethanedithiol/phenol/thioanisole; 90/5/2.5/7.5.5 by volume). The peptides were subsequently filtered and precipitated with cold methyl-tert butyl ether (MTBE). The linear peptides were purified by reversed-phase HPLC using a preparative C_{18} Vydac column (218TP1022). The identity of the peptides was confirmed by mass spectrometry. Oxidative folding was carried out in buffered solution (0.1 M Tris-HCl, pH 7.5) containing 1 mM EDTA, 1 mM reduced, and 1 mM oxidized glutathione. After folding was complete, the reaction was quenched by acidification with formic acid (8% final concentration). The refolded peptides were purified by semipreparative HPLC.

Electrophysiology

Dissociation of DRG Neurons. Frog DRGs were dissected from 2.5 to 3 in. adult *Rana pipiens* of either sex and

dissociated as previously described (*16*). Mouse (Swiss Webster) and rat (Sprague Dawley) DRGs were dissected from adult males and dissociated by essentially the same procedure as that used for the frog DRGs. Briefly, the ganglia were treated with collagenase followed by trypsin. The cells were mechanically dissociated by trituration, washed, and suspended in either of two solutions. The frog solution was 73% Leibowitz's L15 medium supplemented with 14 mM glucose, 1 mM $CaC1_2$, and 7% fetal bovine serum. The mammalian solution was the L15 medium supplemented with 14 mM glucose, 1 mM $CaCl_2$, and 10% fetal bovine serum. Both solutions also contained penicillin/streptomycin. Dissociated DRG neurons were kept in suspension at 4 °C up to a month (frog) or 3 days (mouse and rat).

Whole-Cell Voltage Clamping. The extracellular frog solution was (in mM) NaCl, 117; KCl, 2; $MgCl_2$, 2; $MnCl_2$, 2; HEPES, 5; TEA, 10; pH 7.2. The mammalian extracellular solution was (in mM) NaCl, 140; KCl, 3; $MgCl_2$, 1; $CaCl_2$, 1; HEPES, 20; pH 7.3. To block TTX-sensitive currents, 1 μM TTX was added to these extracellular solutions. Recording pipets had resistances of 1.5 to 2 MΩ, and for frog DRG neurons contained (in mM) NaCl, 10; CsCl, 110; $MgCl_2$, 2; $CaCl_2$, 0.4; EGTA, 4.4; HEPES, 5; TEA, 5; NaATP, 4; pH 7.2. For mammalian DRG neurons, recording pipets contained (in mM) CsF, 140; NaCl, 10; EGTA, 1; HEPES, 10; pH 7.3. These solutions inhibit voltage-gated potassium and calcium currents and thereby permit the recording of only sodium currents. Conotoxins were dissolved in extracellular solution and applied to the neurons under study by bath exchange. Toxin exposures were conducted in static baths. The membrane potential was held at −80 mV, and the sodium channels were activated by a 50 ms test pulse to 0 mV, applied every 20 s. Each test pulse was preceded by a −120 mV prepulse lasting 50 ms. A MultiClamp 700A amplifier (Axon Instruments, Union City, California) was used, and current signals were low-pass filtered at 3 kHz, digitized at a sampling frequency of 10 kHz, and leak-subtracted by a P/6 protocol using in-house software written in LabVIEW (National Instruments, Austin, Texas).

Extracellular Recordings of Action Potentials. Skeletal and heart muscles as well as cutaneous nerves were dissected from the same frogs as those that provided the DRGs. The lateral half of the *cutaneus pectoris* (skeletal) muscle was cut longitudionally into ∼1 mm wide strips, with care taken to damage as few fibers as possible. About six skeletal muscle strips, each about 15 mm long, were isolated from each frog. The wall of the auricle was cut into ∼1 mm wide bands that ran rostro caudally to provide atrial strips, each about 10 mm long. About six such strips were isolated per heart. Nerves innervating the skin of the back were cut at their exit from the back muscle, and at their entry to the dorsal skin, on average each nerve was about $^1/_4$ mm in diameter and about 15 mm long. Each frog provided about six dorsal cutaneous nerves. These preparations were stored in frog Ringer's at 4 °C and used within a week. The recording chamber was fabricated from Sylgard (Dow Chemical, Midland, MI) and consisted of a linear string of three or four wells, each 4 mm in diameter by 4 mm deep (50 μl volume) and separated from its neighbor by a 1 mm wide partition. A bead of Vaseline was placed atop each partition between compartments. The muscle strip or nerve was stretched over the wells and partitions, and each end was pinned with a 0.1 mm diameter stainless steel pin in one or the other outermost well. The skeletal muscle and nerve spanned four wells, whereas the shorter cardiac muscle spanned three wells. Portions of nerve or muscle strip draped over Vaseline were covered with additional Vaseline to prevent drying and seal off compartments from each other such that the fluid in each compartment was isolated and independently maintained. Furthermore, this arrangement allowed electrical stimulation or recording to take place across compartment partitions. Each compartment was maintained as a static bath whose fluid content was refreshed every 15−30 min by manual exchange. Preparations mounted in this fashion provided stable recordings of extracellular action potentials for many hours and could be stored overnight in the refrigerator, if necessary. With nerve and skeletal muscle strip preparations, one stimulating electrode was placed in the first well and the other in the second, and one recording electrode was placed in the third well and one in the fourth. With the atrial strip, which spanned only 3 wells, the arrangement was the same, except that the middle well contained both a recording and stimulating electrode. In all instances, a ground electrode was placed in the second well (or middle well for the atrial strip). Supra maximal stimuli (∼5 V × 0.1 ms, for skeletal muscle; ∼10 V × 0.2 ms, for cardiac muscle; ∼15 V × 1 ms for nerve) were applied once per minute to evoke action potentials. Extracellular action potentials, acquired with a P-55 AC preamplifier (Grass-Telefactor, West Warwick, RI), were band-pass filtered (1 Hz to 1 kHz) and digitized at a sampling frequency of 4 kHz using in-house software written in LabVIEW. All electrodes were stainless steel wires. All compartments contained frog Ringer's solution consisting of (in mM) NaCl, 111; KCl, 2; $CaCl_2$, 1.8; HEPES, 10; pH 7.2. Conotoxins were dissolved in this solution and applied to either the third well (for skeletal muscle strip and nerve) or the middle well (for atrial strip) by replacing its solution with one containing toxin; unless otherwise indicated, toxin-exposures were at least 30 min. All electrophysiological experiments were conducted at room temperature (∼20 °C).

Mouse Bioassays

Conotoxins were delivered to Swiss Webster mice (14−18 day-old) by intracranial (i.c.) injection, as described previously (*17*). The lyophilized peptides were dissolved in normal saline solution and injected using a 29-gauge insulin syringe.

Molecular Modeling

Models were created with the MODELLER (6v2) program (*18*) using the NMR structure of SmIIIA ((*15*), pdb access code 1Q2J, representative structure 13) as a template and the sequence alignments shown in Table 1. From 25 initial models of each peptide, the structure with the lowest modeler objective function was subjected to molecular dynamics (MD) simulation. All MD calculations were performed using the GROMACS (v3.1.4) package of programs (*19*) with the OPLS-aa force field (*20*). Ionizable residues were assumed to be in their standard state at neutral pH. Each peptide was placed in a 40 × 40 × 40 $Å^3$ water box with no pressure coupling. The total charge on the system was made neutral by replacing water molecules with chloride ions using the

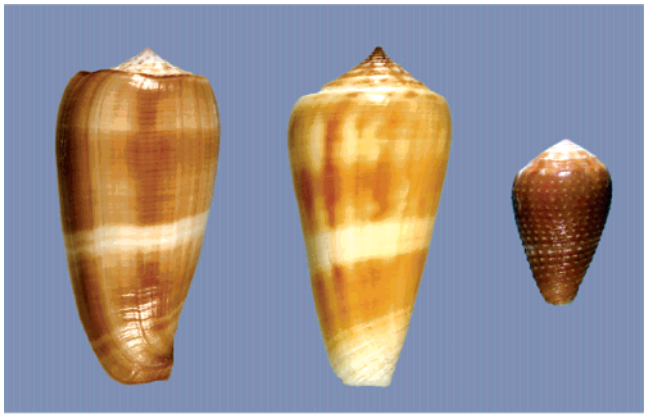

FIGURE 2: Representative shells of snails from which the four new μ-conotoxins were cloned. From left to right: *C. magus*, *C. consors*, and *C. catus*.

Genion program. The LINCS algorithm (*21*) was used to constrain bond lengths. Peptide, water, and ions were coupled separately to a thermal bath at 300 K using a Berendsen thermostat (*22*) applied with a coupling time of 0.1 ps. All simulations were applied with a single nonbonded cutoff of 10 Å, applying a neighbor-list update frequency of 10 steps (20 fs). The particle-mesh Ewald method was applied to deal with long-range electrostatics; a grid width of 1.2 Å was used with a fourth-order spline interpolation. All simulations consisted of an initial minimization of water molecules followed by 100 ps of MD with the fixed peptide. Following positional restraint MD, the restraints on the peptide were removed and the MD simulation continued for a further 100 ps. The time step used in all MD simulations was 2 fs. At the completion of the MD calculation, the system was minimized using the method of steepest descents.

RESULTS

Molecular Cloning and Cladistic Analysis. PCR and cloning of conotoxin genes are well-established techniques to identify novel peptides from any given gene family. We used PCR primers specific for the M-superfamily (*23*) and identified four new μ-conotoxins from the venom of fish-hunting cone snails *Conus consors*, *C. catus*, and *C. magus* (Figure 2). The predicted translation products based on DNA sequences (Table 1, group I) share considerable sequence similarity in the two *C*-terminal loops, which were previously postulated to be important for the recognition of TTX-resistant sodium channels (*15*). Sequence comparison identified three major groups of μ-conotoxins: (I) CIIIA, CnIIIA, CnIIIB, and MIIIA; (II) KIIIA, SIIIA, and SmIIIA; and (III) PIIIA, GIIIA, GIIIB, and GIIIC. Groups I and II shared high sequence similarity in the last two loops, but group I contained in addition a conserved Pro-Asn sequence in the first loop. Among the peptides in these two groups, CnIIIB has the most divergent sequence: it has the Pro-Asn motif, but differs significantly in the second and third loops from other peptides. Analysis of all conotoxins from groups I and II (excluding CnIIIB) yielded the following consensus sequence:

C C $(X)_n$ **C** S X R/K W **C** R D H A/S R/Q **C C**

Because group II peptides have previously been shown to inhibit TTX-resistant sodium channels, the shared-consensus sequence for the last two loops led to the hypothesis that these μ-conotoxins may target TTX-resistant sodium channels. As demonstrated below, this hypothesis was fulfilled when tested experimentally.

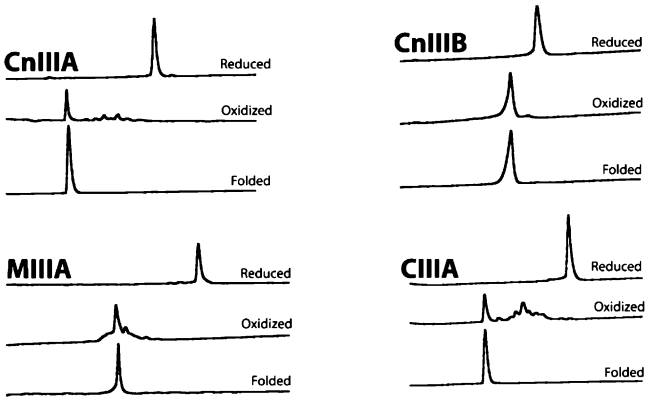

FIGURE 3: Chemical synthesis and oxidative folding of μ-conotoxins. The reduced forms were synthesized on solid support, cleaved from resin, and purified by HPLC prior to folding. Folding reactions were carried out in the presence of reduced and oxidized glutathione in a buffered solution (pH 7.5) at ambient temperature. The HPLC traces represent folding mixtures quenched after 60 min. For all four conotoxins, the steady-state distribution of folding species was established within the first 30 min (not illustrated). The lowest trace in each panel is the chromatogram of the purified folded peptide used for further biological characterizations.

Chemical Synthesis and Oxidative Folding. Chemical synthesis of the four conotoxins in group I was carried out on solid support using standard Fmoc chemistry. The Cys residues were protected by the trityl groups; this synthetic strategy allowed direct oxidation and simultaneous formation of all three disulfide bridges. HPLC-analysis of oxidative folding reactions of all four conotoxins is shown in Figure 3. In most cases, the folding reaction yielded a major product that generally had the shortest retention time relative to the other folding species. This peak was collected and analyzed by mass spectrometry, which indicated that it was fully oxidized. Our previous results with M-superfamily conotoxins had indicated that the folding species with the shortest HPLC retention times were the correctly folded conotoxins (*16*, *24*). The disulfide bond connectivity of the correctly folded μ-conotoxin SmIIIA was previously confirmed using NMR experiments (*15*). The folding and purification protocols were scaled up to produce enough synthetic material for the characterization of the biological activities of the four new μ-conotoxins.

Biological Activities of Four New Conotoxins. The synthetic peptides were first tested on TTX-resistant sodium channels in voltage-clamped frog DRG neurons. As shown in Figure 4, when tested at a concentration of 5 μM, all four peptides blocked TTX-r currents, albeit to different extents. The order of potency was CIIIA > CnIIIA > MIIIA > CnIIIB, with % inhibition (5 μM toxin) ranging between 96 and 25, as shown Table 2. The block by CIIIA, CnIIIA, and MIIIA, similar to that previously shown for KIIIA and SIIIA (*16*), was very slowly reversible, whereas the block by CnIIIB, like that of SmIIIA (*14*), was relatively irreversible (not illustrated). Increasing the concentration of MIIIA to 25 μM resulted in ~80% inhibition. However, increasing CnIIIB concentration from 5 to 50 μM resulted in no significant increase in the level of blocking. The reason for

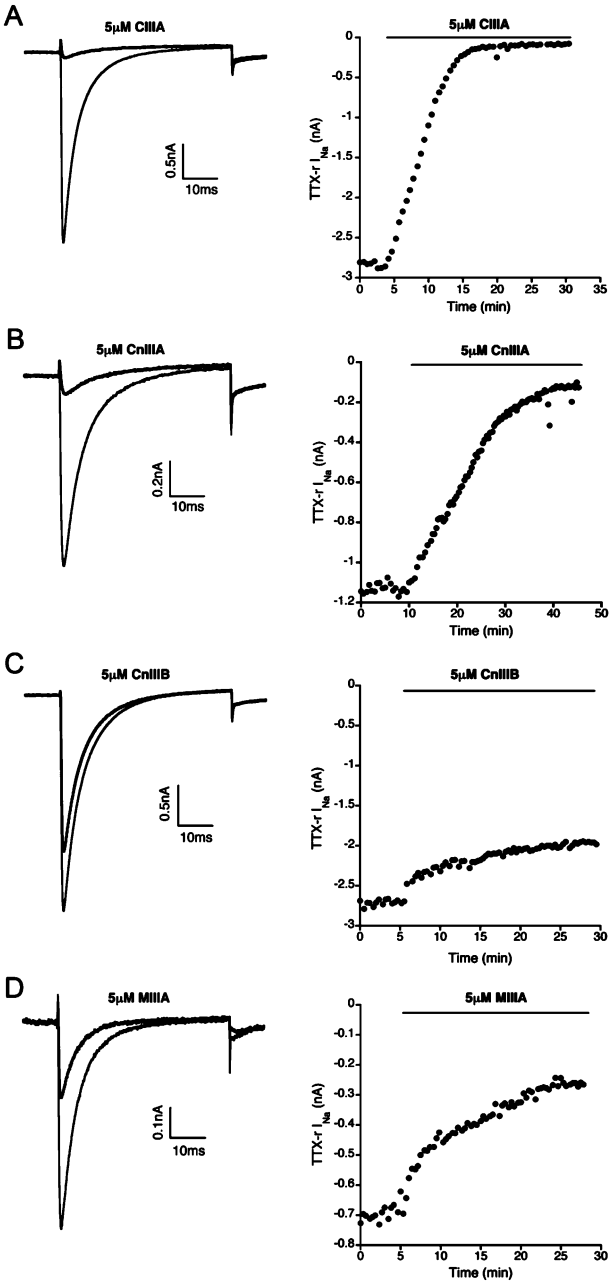

FIGURE 4: Comparison of the blocks by four μ-conotoxins of TTX-resistant sodium currents in frog DRG neurons. Neurons were dissociated and whole-cell voltage clamped as described in Experimental Procedures. Neurons were held at −80 mV, and 50 ms test pulses to 0 mV were applied every 20−30 s, where each test pulse was preceded by a 50 ms prepulse to −120 mV to relieve steady-state inactivation. Each trace represents the average of 10 responses. (A−D) Left column: representative TTX-resistant sodium currents recorded from DRG neurons in the absence of (control traces, gray) or following an ~20 min exposure to 5 μM μ-CIIIA (A), μ-CnIIIA (B), μ-CnIIIB (C), or μ-MIIIA (D). Right column: the peak amplitude of TTX-resistant sodium current plotted as a function of time. The horizontal black line represents the presence of μ-conotoxin.

Table 2: μ-Conotoxin Susceptibility of TTX-Resistant Sodium Currents in Frog DRG Neurons[a]

5 μM μ-conotoxin	TTX-r I_{Na} % block
CnIIIA	87 ± 6
CnIIIB	25 ± 4
CIIIA	96 ± 4
MIIIA	64 ± 12
KIIIA	96 ± 2
SIIIA	91 ± 8
GIIIA	0
PIIIA	8 ± 10

[a] % block of peak TTX-r I_{Na} following 25−30 min of exposure to 5 μM μ-conotoxin (mean ± SD, $N = 3$ to 5).

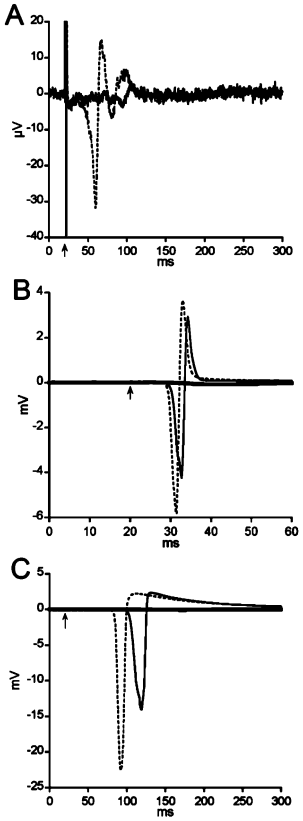

FIGURE 5: μ-Conotoxin CIIIA blocks action potentials in three different preparations of frog solutions. The action potentials were recorded extracellularly as described in Experimental Procedures. (A) TTX-resistant C-CAPs in cutaneous nerve. Average of four responses before (.....) and after 60 min of exposure to 3 μM CIIIA (−). The stimulus was applied at 20 ms (arrow), eliciting a two-component C-CAP that was largely blocked after toxin-exposure. TTX (1 μM) was present throughout. (B) Action potential in skeletal muscle before (.....) and after 50 min in 1 μM CIIIA (thin solid trace) and after CIIIA was increased to 3 μM for 30 min (bold solid trace). (C) Cardiac-muscle action potential before (.....) and after 120 min in 1 μM CIIIA (thin solid trace) and after CIIIA concentration had been increased to 3 μM for 30 min (—). For both muscles, CIIIA at 1 μM slowed the action potential, and at 3 μM, obliterated it. The stimulus was applied at 20 ms (arrow).

this is not understood, and experiments are in progress to resolve this issue. Table 2 also compares the activities of the four new μ-conotoxins with those belonging to groups II and III. As summarized in the Table, only μ-conotoxins belonging to group I and II exhibited significant antagonist activity against TTX-r sodium channels in frog DRG neurons. The most potent conotoxins from group I, namely CnIIIA and CIIIA, were chosen to carry out extensive functional characterization with respect to a selectivity profile and their activity against mammalian sodium channels.

Characterization of CnIIIA and CIIIA. To determine the selectivity for CnIIIA and CIIIA on different sodium channels, extracellular recordings of action potentials were obtained from three isolated tissue preparations from frog: skeletal muscle, cardiac muscle, and cutaneous nerves.

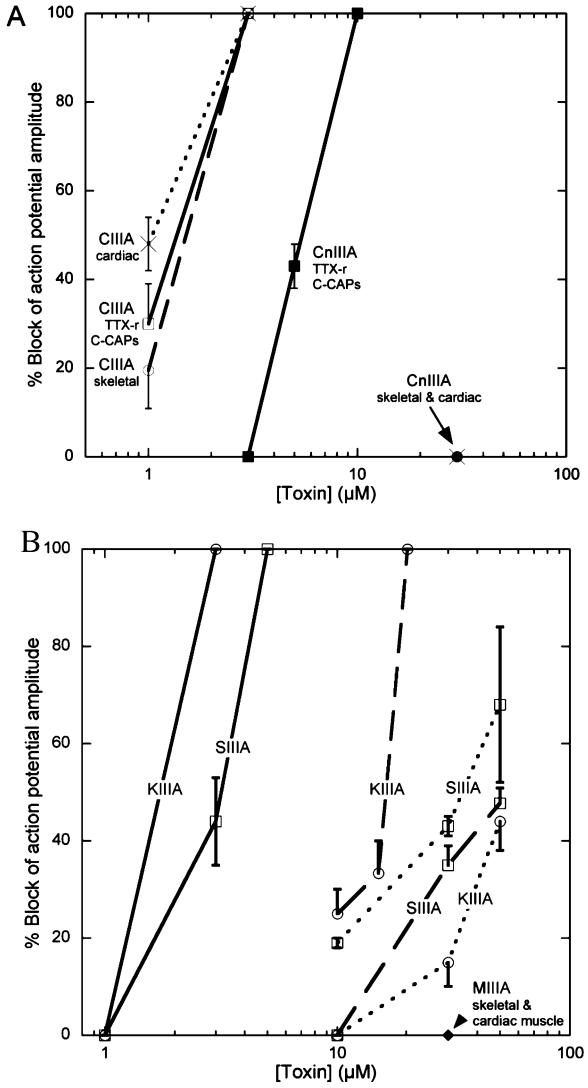

FIGURE 6: Dose-dependencies of blocks by μ-conotoxins CIIIA and CnIIIA (panel A) and SIIIA and MIIIA (panel B) of action potentials in three preparations of frog solutions. Extracellular recordings were made as described in Experimental Procedures (Figure 5). (A) Block by CIIIA of action potentials in cardiac muscle (X's), skeletal muscle (○), and TTX-resistant C-CAPs in nerve (□). Block by CnIIIA of TTX-r C-CAPs (■), and at 30 μM, the highest concentration tested, CnIIIA had no effect on the action potentials in both muscles (X and ●). Thus, although CnIIIA was less potent than CIIIA in blocking TTX-r C-CAPs, it was more specific in so far as it had no effects on action potentials in the two-muscle preparations. (B) Block by KIIIA (○) and SIIIA (□) of TTX-r C-CAPs (−), skeletal muscle action potentials (----), and cardiac muscle action potentials (.....). MIIIA was only tested at 30 μM on cardiac and skeletal muscles, where it had no observable effect (♦). For both panels, each point represents mean ± SE of three preparations. The blocks of cardiac- and skeletal-muscle action potentials were reversed within 60 min of washout for all toxins. The reversibility of the block of TTX-r C-CAPs was tested only for CIIIA. An overnight wash was required for full recovery.

Because our previous studies indicated that SIIIA could block compound action potentials of C-fibers (C-CAPs) that persist in the presence of TTX (*16*), TTX was included in the experiments with nerve preparation.

Figure 5A illustrates representative recordings from a TTX-treated nerve and shows that 3 μM CIIIA largely blocked TTX-r C-CAPs. Sample recordings of action potentials in frog skeletal and cardiac muscles are shown in Figure 5B and C, which show that 3 μM CIIIA also obliterates action potentials in these muscles. For each μ-conotoxin, the block of action potentials in all three tissues was determined at varying concentrations to produce dose−response profiles. The profiles for CnIIIA and CIIIA are illustrated in Figure 6A.

Table 3: Selectivity Profile of μ-Conotoxins on the Basis of Their Ability to Block Action Potentials in the Three Preparations from *Rana pipiens*[a]

conotoxin	skeletal muscle	cardiac muscle	nerve C-CAP (in TTX)
CnIIIA	−	−	+
CIIIA	+	+	+
MIIIA	−	−	n.t.
previously described peptides			
KIIIA	+/−[b]	+/−	+[b]
SIIIA	+/−[b]	+/−	+[b]
GIIIA	+[c]	−	−
PIIIA	+[d]	−	−
SmIIIA	+[b]	n.t.	+[b]

[a] Unless indicated otherwise, data are from Figure 6. +, estimated IC_{50} lower than 10 μM; −, estimated IC_{50} higher than 50 μM; +/−, IC_{50} in the 10−50 μM range; and n.t, not tested. [b] Bulaj et al., 2005. [c] Cruz et al., 1985. [d] Shon et al., 1998.

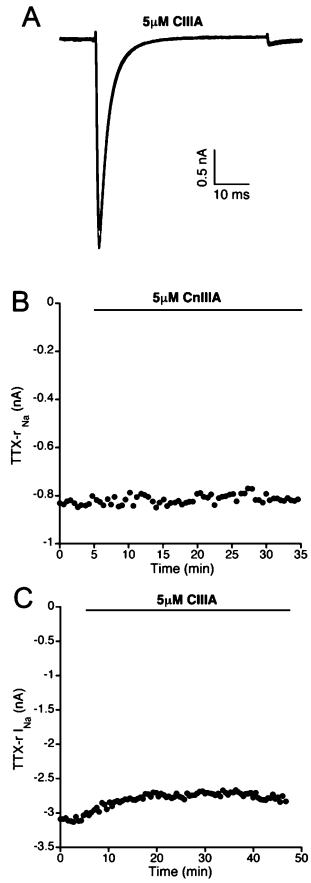

FIGURE 7: Comparison of the effects of μ-conotoxins on TTX-resistant sodium currents in mouse DRG neurons. Neurons were dissociated and whole-cell voltage clamped as described in Experimental Procedures. The same voltage clamp protocol as in Figure 4 was used with 1 μM TTX present throughout the experiment. (A) Representative TTX-resistant sodium current before (control, gray trace) and after a 40 min exposure to CIIIA (black trace). Each trace represents the average of 10 responses. (B−C) Peak amplitude of TTX-resistant sodium current plotted as a function of time. The horizontal black line represents the presence of 5 μM CIIIA (B) or 5 μM CnIIIA (C).

Table 4: Mouse Bioassay Results for CnIIIA and CIIIA, Following i.c. Administration[a]

μ-conotoxin	dose (nmol/g)	behavioral effects
CnIIIA	0.7	no notable effects.
	0.9	3 min after injection, light seizure followed by random run/pause; 5 min, intermittent grand mal seizures begin, subjects continued to squeak throughout; seizures continued without recovery.
	1.5	immediate lethargy following injection; 3 min after injection, slight dyskinesia, and the subjects were lying in place with little to no movement; 5 min, stage II seizure; intermittent seizures continued without recovery.
	1.7	immediate lethargy following injection; 3 min after injection, stage II seizure; 5 min, grand mal seizure (full body); seizures continued intermittently until death at 14 min.
CIIIA	0.2	lethargy and allodynia 4 min after injection; 15 min, slight weakness/dyskinesia; complete paralysis at 37 min; slight recovery from paralysis at 3 h.
	0.3	lethargy 2 min after injection; 4 min, slight trembling; 8 min, slight weakness/dyskinesia; 12 min, increasing dyskinesia/weakness; complete paralysis at 20 min;
	0.5	immediate lethargy following injection; 4 min after injection weakness/dyskinesia; 6 min, increasing weakness/dyskinesia; full paralysis at 8 min; death at 13 min due to respiratory failure as noted by subjects' blue/purple color and tendency to gasp for air.
	0.55	immediate lethargy following injection and hypersensitivity to touch; 2 min, stage II seizure; 5−8 min, death.

[a] One mouse per dose was used in these experiments.

To compare the selectivity profiles of CnIIIA and CIIIA to those of previously characterized μ-conotoxins, we also determined similar profiles for a few selected peptides. Previously, profiles for KIIIA and SIIIA were obtained only on skeletal muscle and over a more limited concentration range (*16*). In Figure 6B shows the profiles of KIIIA and SIIIA. The availability of MIIIA was limited, so it was only tested on cardiac and skeletal muscles where it had no observable effect at a concentration of 30 μM (Figure 6B). Group III peptides, PIIIA and GIIIA, which readily block skeletal-muscle action potentials, have not been tested previously on TTX-r C-CAPs and cardiac action potentials. When tested at a concentration of 30 μM, both peptides blocked neither TTX-r C-CAPs nor cardiac action potentials (not illustrated).

Tabulated in Table 3 are the IC_{50} ranges of eight μ-conotoxins estimated from the data in Figure 6 and the results of previous reports (see Table for references). As shown in Table 3, CnIIIA is quite selective for TTX-r channels, whereas CIIIA is pan-specific. The selectivity profiles of KIIIA and SIIIA were similar to each other. On the basis of these results, the selectivity of μ-conotoxins was as follows (starting with the most selective against TTX-resistant sodium channels): CnIIIA > SIIIA ∼ KIIIA > SmIIIA ∼ CIIIA. The two new peptides, CnIIIA and CIIIA, were also tested on TTX-r currents in mouse and rat DRG neurons. Figure 7 shows that these peptides blocked TTX-r currents in mouse DRG neurons only poorly at best. In contrast to the ∼90% block of TTX-r currents in frog DRG neurons by 5 μM CnIIIA and CIIIA (Table 2), the concentration of these peptides reduced TTX-r currents in mouse DRG neurons negligibly (CnIIIA) or only by about 10% (CIIIA). Similar results were obtained with recordings from rat DRG neurons (not illustrated). Thus, μ-conotoxins exhibit a significant difference in potency against TTX-r currents, depending on the animal species the DRG neurons were derived from.

In contrast to the low apparent potency in blocking TTX-resistant currents in mammalian DRG neurons, μ-conotoxins produced a range of behavioral responses when injected intracranially into mice. As shown in Table 4, both peptides induced seizures, but only CIIIA caused a long-lasting paralysis even at a dose of 200 pmol/g. However, the most selective blocker of frog TTX-r channels, CnIIIA, produced only seizures when tested at doses of 1.5 nmol/g. These results suggest that despite the relatively low activity of μ-conotoxins on rat and mouse TTX-r sodium channels, these peptides appear to have different biological activities in the mammalian CNS. Our preliminary results indicated that 10 μM CnIIIA competed in a binding assay with saxitoxin using rat-brain-membrane preparations (G. Bulaj, unpublished data). Studies are in progress to determine the structural factors responsible for these interspecies differences and to define the differences in sodium channel subtype selectivity in mammalian systems. The observation that these peptides cause seizures was unexpected.

Molecular Modeling of μ-Conotoxins. To gain greater insight into the structural features of μ-conotoxins from groups I and II, homology modeling was carried out for CnIIIA, CnIIIB, CIIIA, and MIIIA. Using the pdb coordinates of SmIIIA and methods previously described for modeling KIIIA and SIIIA (*16*), model structures were generated. Models of μ-conotoxin structures are illustrated in Figure 8.

Because all models were on the basis of the SmIIIA template, the general topology of each model structure is very similar. However, examination of the structures of two selective μ-conotoxins, CnIIIA and KIIIA, highlights an additional structural feature unique to these μ-conotoxins. The superposition of the structures of CnIIIA and KIIIA yields asparagine residues Asn8 and Asn3, respectively (indicated by an arrow in Figure 8), that occupy the same spatial position. In nonselective CIIIA from group I, the side-chain amide of Asn8 forms a hydrogen bond with the

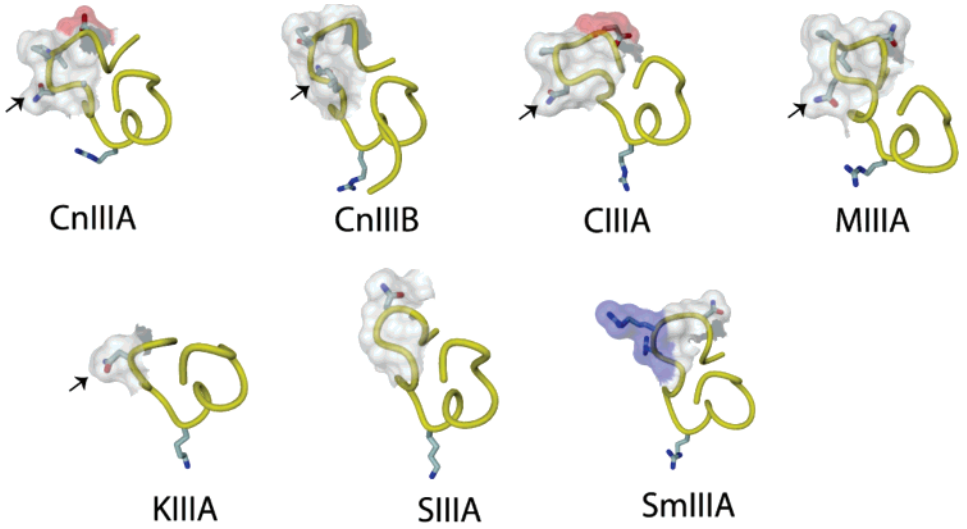

FIGURE 8: Homology modeling of μ-conotoxins targeting TTX-resistant sodium channels. The surface of the first loop is highlighted, and the side chain of the positively charged Lys/Arg in the second loop is shown at the bottom of each structure. The models were generated on the basis of the structure of μ-SmIIIA determined by NMR. The asparagine residues are indicated with an arrow. The graphics were generated using the 3D visualization program DINO (Visualizing Structural Biology (2002) http://www.dino3d.org). Model coordinates are available (Supporting Information).

backbone carbonyl of Gly6; coinciding with this H-bond is another hydrogen bond between the amide NH of Asn8 and the backbone carbonyl of Cys3, which brings the side-chain atoms of Pro7 and Cys3 in close contact. These hydrogen bonds are precluded from forming in CnIIIA by the bulky side chain of Val6; in CIIIA this residue is a glycine. These interactions sequester the side chain of Asn8 in CIIIA and prevent it from occupying the site observed above in CnIIIA.

The μ-conotoxin KIIIA contains only a single residue in the first loop, and represents the largest structural deviation from the model template. Preservation of the position of disulfide linkages from the template in the model results in the superposition of Asn3 of KIIIA with Asn8 of CnIIIA and the coincidence of their side chains. In the nonselective μ-conotoxin SmIIIA from Group II, the sequence-equivalent asparagine to Asn3 in KIIIA (N5) is located ~9 Å (Cα−Cα distance) from the asparagine residues of the selective μ-conotoxins. The role of these asparagine residues in the blocking of TTX-r sodium channels by μ-conotoxins remains to be elucidated.

DISCUSSION

There is a continuing interest in the discovery of antagonists of sodium channels with novel subtype selectivity. The work presented here investigated a group of sodium channel-targeting peptide toxins from fish-hunting *Conus* snails that have in common two characteristic structural features: (i) sequence homology within the two *C*-terminal loops, and (ii) a Pro-Asn motif in the first loop. The first structural feature, previously described for the three μ-conotoxins SmIIIA, SIIIA, and KIIIA, suggested that the new peptides might target TTX-r sodium channels. Indeed, all four conotoxins were able to block TTX-r sodium currents in frog DRG neurons, but one, CnIIIB, was far less effective than the others. At the concentrations tested, it also did not block compound TTX-r action potentials (data not shown). Moreover, these new μ-conotoxins exhibited strikingly different selectivities, from the highly selective CnIIIA, which was a specific antagonist for frog TTX-r sodium channels, to the nonselective CIIIA. Thus, the targeting specificity of the new peptides is remarkably divergent, despite the considerable sequence similarity between CnIIIA and CIIIA, including the Pro-Asn motif in the first loop.

Highly selective CnIIIA and nonselective CIIIA differ from each other by four nonconservative substitutions. Interestingly, these four substituted CIIIA residues (Gly6, Gly9, Ser12, and Arg20) are also found in another nonselective μ-conotoxin, SmIIIA. Because the residues Ser12 and Arg20 are present in selective μ-conotoxins KIIIA and SIIIA, this leaves, by deduction, only two residues, Gly 6 and Gly 9, in the first loop accountable for a change in the selectivity profile. On another note, molecular modeling suggested that asparagine residues located in the first loop may play a role in interactions with sodium channels. Taken together, all of these observations suggest a series of amino acid replacements in CnIIIA and CIIIA to better understand the structural determinants of their selectivites.

It is not surprising that even minimal changes in a primary sequence may affect the selectivity of μ-conotoxins. Such subtle effects were previously described for GIIIA and GIIIB conotoxins (Table 1). These two peptides differ only in two amino acid positions from each other, but they appear to discriminate between mutated $Na_v1.4$ sodium channel subtypes (*25*, *26*). Because interactions between μ-conotoxins GIIIA and $Na_v1.4$ sodium channels have been extensively studied using mutagenesis (*27*−*30*), it is likely that similar structural studies will follow in the case of μ-conotoxins from groups I and II and their molecular targets.

The major cardiac sodium channel in mammals, Na_V 1.5, is relatively TTX-resistant (IC_{50} 2 μM) (*31*). In contrast, the cardiac action potential of *Rana pipiens* frogs used in this study is very sensitive to TTX (IC_{50} ~5 nM), as is the skeletal-muscle action potential of these frogs (IC_{50} ~10 nM) (Fiedler and Yoshikami, unpublished data). This raises the possibility that the same sodium channels might be responsible for the action potentials in both cardiac and skeletal muscles in frogs. However, this is belied by the observation

that skeletal- but not cardiac-muscle action potentials are readily blocked by GIIIA and PIIIA (Table 3). Furthermore, the skeletal muscle is slightly more sensitive than the cardiac muscle to KIIIA, whereas the converse is true with SIIIA (Figure 6B). Thus, the cardiac and skeletal muscles of frogs have pharmacologically distinct sodium channels, most likely a reflection of the two muscles possessing different channel isoforms, as is the case not only in mammals but also in fish (*32*).

The new μ-conotoxins add to an emerging molecular diversity in this gene family. Presently, 11 distinct μ-conotoxins have been characterized from 8 fish-hunting *Conus* species. Because all of these peptides were chemically synthesized and functionally characterized, this allowed a better structural and functional definition of the μ-conotoxin family. In addition to a high conservation of positively charged residues, the most conserved amino acid in the peptides in group I and II is the Trp residue located in the second loop. This residue was first suggested to play a potential role in the interactions with TTX-r sodium channels (*15*). As summarized in Table 1, groups I and II comprise peptides targeting amphibian sodium channels with divergent selectivity; SmIIIA and CIIIA are about equipotent in blocking skeletal muscle TTX-sensitive channels and sensory TTX-r channels, whereas CnIIIA is highly selective for TTX-r channels. Their subtype selectivity against mammalian sodium channel subtypes remains to be fully characterized, but our results indicate that at least some of these peptides are active in the mammalian CNS. Taken together, these two groups of μ-conotoxins provide a unique opportunity to develop novel pharmacological tools for sodium channels.

ACKNOWLEDGMENT

We thank Jacob S. Nielsen, Jessica Kranski, and Erika Fuller for their help and technical assistance with peptide synthesis.

SUPPORTING INFORMATION AVAILABLE

Protein data bank model coordinates for compounds discussed in this article. This material is available free of charge via the Internet at http://pubs.acs.org.

REFERENCES

1. Goldin, A. L. (1999) Diversity of mammalian voltage-gated sodium channels, *Ann. N.Y. Acad. Sci. 868*, 38−50.
2. Goldin, A. L. (2001) Resurgence of sodium channel research, *Annu. Rev. Physiol. 63*, 871−894.
3. Waxman, S. G., Cummins, T. R., Dib-Hajj, S., Fjell, J., and Black, J. A. (1999) Sodium channels and pain, *Proc. Natl. Acad. Sci. U.S.A. 96*, 7635−7639.
4. Waxman, S. G., Cummins, T. R., Dib-Hajj, S., Fjell, J., and Black, J. A. (1999) Sodium channels, excitability of primary sensory neurons, and the molecular basis for pain, *Muscle Nerve 22*, 1177−1187.
5. Wood, J. N., Boorman, J. P., Okuse, K., and Baker, M. D. (2004) Voltage-gated sodium channels and pain pathways, *J. Neurobiol. 61*, 55−71.
6. Novakovic, S. D., Eglen, R. M., and Hunter, J. C. (2001) Regulation of Na+ channel distribution in the nervous system, *Trends Neurosci. 24*, 473−8.
7. French, R. J., and Terlau, H. (2004) Sodium channel toxins−receptor targeting and therapeutic potential, *Curr. Med. Chem. 11*, 3053−3064.
8. Terlau, H., and Olivera, B. M. (2004) *Conus* venoms: a rich source of novel ion channel-targeted peptides, *Physiol. Rev. 84*, 41−68.
9. McIntosh, J. M., Hasson, A., Spira, M. E., Gray, W. R., Li, W., Marsh, M., Hillyard, D. R., and Olivera, B. M. (1995) A new family of conotoxins that blocks voltage-gated sodium channels, *J. Biol. Chem. 270*, 16796−16802.
10. Cruz, L. J., Gray, W. R., Olivera, B. M., Zeikus, R. D., Kerr, L., Yoshikami, D., and Moczydlowski, E. (1985) *Conus geographus* toxins that discriminate between neuronal and muscle sodium channels, *J. Biol. Chem. 260*, 9280−9288.
11. Cruz, L. J., Kupryszewski, G., LeCheminant, G. W., Gray, W. R., Olivera, B. M., and Rivier, J. (1989) μ-Conotoxin GIIIA, a peptide ligand for muscle sodium channels: chemical synthesis, radiolabeling and receptor characterization, *Biochemistry 28*, 3437−3442.
12. Safo, P., Rosenbaum, T., Shcherbatko, A., Choi, D., Han, E., Toledo-Aral, J., Olivera, B. M., Brehm, P., and Mandel, G. (2000) Distinction among neuronal subtypes of voltage-activated sodium channels by μ-conotoxin PIIIA, *J. Neurosci. 20*, 76−80.
13. Nielsen, K. J., Watson, M., Adams, D. J., Hammarström, A. K., Gage, P. W., Hill, J. M., Craik, D. J., Thomas, L., Adams, D., Alewood, P. F., and Lewis, R. J. (2002) Solution structure of μ-conotoxin PIIIA, a preferential inhibitor of persistent tetrodotoxin-sensitive sodium channels, *J. Biol. Chem. 277*, 27247−27255.
14. West, P. J., Bulaj, G., Garrett, J. E., Olivera, B. M., and Yoshikami, D. (2002) μ-Conotoxin SmIIIA, a potent inhibitor of TTX-resistant sodium channels in amphibian sympathetic and sensory neurons, *Biochemistry 41*, 15388−15393.
15. Keizer, D. W., West, P. J., Lee, E. F., Yoshikami, D., Olivera, B. M., Bulaj, G., and Norton, R. S. (2003) Structural basis for tetrodotoxin-resistant sodium channel binding by μ-conotoxin SmIIIA, *J. Biol. Chem. 278*, 46805−46813.
16. Bulaj, G., West, P. J., Garrett, J. E., Marsh, M., Zhang, M.-M., Norton, R. S., Smith, B. J., Yoshikami, D., and Olivera, B. M. (2005) Novel conotoxins from *Conus striatus* and *Conus kinoshitai* selectively block TTX-resistant sodium channels, *Biochemistry 44*, 7259−7265.
17. Clark, C., Olivera, B. M., and Cruz, L. J. (1981) A toxin from *Conus geographus* venom which acts on the vertebrate central nervous system, *Toxicon 19*, 691−699.
18. Fiser, A., and Sali, A. (2003) Modeller: generation and refinement of homology-based protein structure models, *Methods Enzymol. 374*, 463−493.
19. Lindahl, E., Hess, B., and van der Spoel, D. (2001) Gromacs 3.0: a package for molecular simulation and trajectory analysis, *J. Mol. Model. 7*, 306−317.
20. Jorgensen, W. L., and Tirado-Rives, J. (1988) The OPLS potential functions for proteins. Energy minimizations for crystals of cyclic peptides and crambin, *J. Am. Chem. Soc. 110*, 1657−1666.
21. Hess, B., Bekker, H., and Berendsen, H. J. C. (1977) LINCS: a linear constraint solver for molecular simulations, *J. Comput. Chem. 18*, 1463−1472.
22. Berendsen, H. J. C., Postma, J. P. M., DiNola, A., and Haak, J. R. (1984) Molecular dynamics with coupling to an external bath, *J. Chem. Phys. 81*, 3684−3690.
23. Corpuz, G. P., Jacobsen, R. B., Jimenez, E. C., Watkins, M., Walker, C., Colledge, C., Garrett, J. E., McDougal, O., Li, W., Gray, W. R., Hillyard, D. R., Rivier, J., McIntosh, J. M., Cruz, L. J., and Olivera, B. M. (2005) Definition of the M-conotoxin superfamily: characterization of novel peptides from molluscivorous *Conus* venoms, *Biochemistry 44*, 8176−8186.
24. Fuller, E., Green, B. R., Catlin, P., Buczek, O., Nielsen, J. S., Olivera, B. M., and Bulaj, G. (2005) Oxidative folding of conotoxins sharing an identical disulfide bridging framework, *FEBS J. 272*, 1727−1738.
25. Cummins, T. R., Aglieco, F., and Dib-Hajj, S. D. (2002) Critical molecular determinants of voltage-gated sodium channel sensitivity to μ-conotoxins GIIIA/B, *Mol. Pharmacol. 61*, 1192−1201.
26. Li, R. A., Ennis, I. L., Tomaselli, G. F., French, R. J., and Marban, E. (2001) Latent specificity of molecular recognition in sodium channels engineered to discriminate between two "indistinguishable" μ-conotoxins, *Biochemistry 40*, 6002−6008.
27. Dudley, S. C., Jr., Chang, N., Hall, J., Lipkind, G., Fozzard, H. A., and French, R. J. (2000) μ-conotoxin GIIIA interactions with the voltage-gated Na(+) channel predict a clockwise arrangement of the domains, *J. Gen. Physiol. 116*, 679−690.
28. Dudley S. C., Jr., Todt, H., Lipkind, G., and Fozzard, H. A. (1995) A μ-conotoxin-insensitive Na^+ channel mutant: possible localization of a binding site at the outer vestibule, *Biophys. J. 69*, 1657−1665.

29. Dudley S. C., Jr., Chang, N., Hall, J., Lipkind, G., Fozzard, H. A., and French, R. J. (2000) μ-Conotoxin GIIIA interactions with the voltage-gated Na^+ channel predict a clockwise arrangement of the domains, *J. Gen. Physiol. 116*, 679−689.
30. Li, R. A., Ennis, I. L., French, R. J., Dudley, S. C., Jr., Tomaselli, G. F., and Marban, E. (2001) Clockwise domain arrangement of the sodium channel revealed by (μ)-conotoxin (GIIIA) docking orientation, *J. Biol. Chem. 276*, 11072−11077.
31. White, M. M., Chen, L. Q., Kleinfield, R., Kallen, R. G., and Barchi, R. L. (1991) SkM2, a Na+ channel cDNA clone from denervated skeletal muscle, encodes a tetrodotoxin-insensitive Na+ channel, *Mol. Pharmacol. 39*, 604−608.
32. Lopreato, G. F., Lu, Y., Southwell, A., Atkinson, N. S., Hillis, D. M., Wilcox, T. P., and Zakon, H. H. (2001) Evolution and divergence of sodium channel genes in vertebrates, *Proc. Natl. Acad. Sci. U.S.A. 98*, 7588−7592.
33. Shon, K., Olivera, B. M., Watkins, M., Jacobsen, R. B., Gray, W. R., Floresca, C. Z., Cruz, L. J., Hillyard, D. R., Bring, A., Terlau, H., and Yoshikami, D. (1998) μ-Conotoxin PIIIA, a new peptide for discriminating among tetrodotoxin-sensitive Na channel subtypes, *J. Neurosci. 18*, 4473−4481.

BI052162J